Analysis of Coupled Cylindrical Striplines Filled with Multilayered Dielectrics

C. JAGADESWARA REDDY AND MANOHAR D. DESHPANDE

Abstract—**A method of analysis for coupled cylindrical striplines filled with multilayered dielectrics is presented using a variational technique in the space domain. Coupled mode analysis is presented for the case of a pair of coupled circular arc strips arbitrarily located between cylindrical ground planes filled with multilayered dielectrics. An even- and odd-mode approach is used for the analysis of shielded cylindrically curved edge-coupled pairs of broad-side parallel strips (broad-side, edge-coupled cylindrical striplines). The effect of environmental changes on an otherwise planar structure is also studied by extending the present analysis to cylindrically warped coupled striplines.**

I. INTRODUCTION

IN THE RECENT past, investigations on cylindrical striplines and microstrip lines have been reported in the literature [1]–[9]. These lines can be used for applications such as transition adapters, baluns, and slotted lines [5]. In addition to these applications, these lines can be used to excite printed antennas on cylindrical surfaces. Analysis of cylindrical and cylindrically warped striplines by a seminumerical solution of the Laplace equation was presented by Wang [1]. Joshi *et al.* determined the characteristic impedance of homogeneously filled cylindrical striplines by residue calculus technique [2] and also by conformal transformations [3]. Das *et al.* [4] presented the impedance characteristics of cylindrical striplines filled with multilayered dielectrics. Zeng *et al.* [5] found closed-form expressions for characteristic impedances of cylindrical striplines with zero and finite thicknesses. The present authors obtained a simplified closed-form expression for the characteristic impedance of cylindrical stripline with multilayered dielectrics [6]. Due to their usage in exciting an array of patch antennas on cylindrical surfaces, it is worthwhile to study the coupled cylindrical striplines. Coupled cylindrical striplines were investigated by Das *et al.* [7] in the space domain using a variational technique, with grounded electric walls placed on both sides of the coupled strips. Recently, analysis of a class of cylindrical multiconductor transmission lines was done by Chan *et al.* [8] using an iterative approach. Spectral-domain analysis of coupled cylindrical striplines symmetrically placed with equal angular widths was done by the authors to obtain the even- and odd-mode characteristic impedances [9].

In this paper, two different types of coupled cylindrical stripline structures with multilayered dielectrics have been analyzed. First, a method for calculating the mutual coupling between two cylindrical strips with equal or unequal angular widths and arbitrarily located between two grounded cylinders with multilayered dielectrics is presented. Assuming TEM mode propagation, a generalized expression for coupling between a pair of coupled cylindrical striplines is obtained in terms of coefficients of magnetic coupling k_L and capacitive coupling k_C [10]. The magnetic and capacitive coupling coefficients are determined from an evaluation of the mutual parameters L_m and C_m and the primary constants L_1, C_1, L_2, and C_2 of the strips, where the subscripts 1 and 2 stand for the first and second strips, respectively. The primary constants of each strip are determined separately in the absence of the other strip from the Green's function formulation and the assumption of a suitable charge distribution on the strip [4]. The mutual parameters are obtained by calculating the magnetic and electric energies with the two strips present [13]. The even- and odd-mode impedances for coplanar cylindrical strips with equal widths are calculated using coupling coefficients [10] and are compared with those calculated using spectral-domain analysis [9]. Numerical results on coplanar and noncoplanar cylindrical strips are presented. The general formulation for cylindrical striplines is extended to the case of cylindrical microstrip lines by assuming that the outer grounded cylinder is moved to infinity.

Second, a method of analysis for a broad-side, edge-coupled cylindrical stripline structure with layered dielectric is presented. These coupled transmission lines can support several propagating modes. In order to study the electric response produced by these coupled transmission lines for various excitations, a knowledge of characteristic impedances and effective dielectric constants for all possible modes is essential. In this work, the three-layer, broad-side, edge-coupled cylindrical stripline structure is analyzed using a variational technique in the space domain. Assuming that the transverse dimensions of the structure are small compared to the operating wavelength, a quasi-TEM-mode approximation is used for the analysis. From the solution of the two-dimensional Laplace equation in cylindrical coordinates, the potential distribution function

Manuscript received July 11, 1987; revised February 29, 1988.

C. J. Reddy was with Radar and Communication Centre, Indian Institute of Technology, Kharagpur-721 302, India. He is now with the Society for Applied Microwave Electronics Engineering and Research (SAMEER), IIT Campus, Powai, Bombay-400076, India.

M. D. Deshpande is with the NASA-Langley Research Center, Hampton, VA 23665, on leave from the Department of Electronics and Electrical Communication Engineering, Indian Institute of Technology, Kharagpur-721 302, India.

IEEE Log Number 8822326.

0018-9480/88/0900-1301$01.00 ©1988 IEEE

$\psi(\rho,\phi)$ is found. Variational expressions for different mode capacitances are found assuming a suitable charge distribution on the conducting strips. The characteristic impedances and effective dielectric constants of all possible propagating modes are computed. The coupled line structures presented in this work can be used as building blocks for directional couplers, filters, and other important transmission line devices on cylindrical surfaces.

The cases of cylindrically warped coupled striplines are also studied. Their impedances are obtained from the coupled cylindrical stripline solutions by letting the radii of the cylinders be very large and a maintaining the finite arc length of the strip and finite line height, and a comparison with their planar counterparts is made.

II. Coupled Mode Analysis of a Pair of Coupled Cylindrical Striplines

Consider the structure of the single cylindrical stripline shown in Fig. 1(a) along with the notations to be followed. Assuming TEM mode propagation, the characteristic impedance of the stripline can be determined from the expression

$$Z_{c1}=\frac{1}{v_0\sqrt{C_1C_{a1}}}=\sqrt{\frac{L_1}{C_1}} \tag{1}$$

where v_0 is the velocity of light in free space, C_1 is the capacitance per unit length of the structure with multilayered dielectrics, C_{a1} is capacitance per unit length of the structure with $\epsilon_{r1}=\epsilon_{r2}=\epsilon_{r3}=1.0$, and L_1 is the inductance per unit length. The variational expression for capacitance C_1 is given by [12]

$$\frac{1}{C_1}=\frac{\int\int q_1(b,\phi)q_1(b,\phi')G_1(\rho,\phi/b,\phi')b\,d\phi\,d\phi'}{\left[\int q_1(b,\phi)b\,d\phi\right]^2} \tag{2}$$

where $q_1(b,\phi)$ is the charge distribution on the circular arc strip, and $G_1(\rho,\phi/b,\phi')$ is the Green's function of the problem. The potential distribution function $\psi_1(\rho,\phi)$ can be determined from the formula

$$\psi_1(\rho,\phi)=\int_{\text{strip}} G_1(\rho,\phi/b,\phi')q_1(b,\phi')b\,d\phi'. \tag{3}$$

Considering the field singularity at the edges of the strip, the expression for charge distribution appearing in (2) can be assumed as

$$q_1(b,\phi)=\frac{Q_0}{\sqrt{1-\left[\dfrac{(\phi-\theta_{01})}{\alpha_1}\right]^2}} \qquad \theta_{01}-\alpha_1\leqslant\phi\leqslant\theta_{01}+\alpha_1$$

$$=0 \qquad \text{otherwise} \tag{4}$$

where Q_0 is a constant.

For a TEM mode approximation the potential function satisfies the two-dimensional Poisson's equation in cylindrical coordinates [4]:

$$\nabla^2\psi_1(\rho,\phi)=-q(b,\phi)/\epsilon \tag{5}$$

where ϵ is the dielectric constant. Solving (5) and applying proper boundary conditions [4], Green's function due to a unit line charge placed at (b,ϕ') is obtained for different regions as

$$G_1(\rho,\phi/b,\phi)=\frac{\ln\rho/a}{2\pi\epsilon_0 I_0}\epsilon_{r2}\ln c/b$$
$$+\sum_{n=1}^{\infty}\frac{\sinh(n\ln\rho/a)}{n\pi\epsilon_0 D_{n1}}\epsilon_{r2}\sinh(n\ln c/b)$$
$$\cdot\cos n(\phi-\theta_{01})\cos n(\phi'-\theta_{01})$$
$$\text{for } a\leqslant\rho\leqslant d \tag{6}$$
$$=\frac{\ln c/b}{2\pi\epsilon_0 I_0}[\epsilon_{r1}\ln\rho/d+\epsilon_{r2}\ln d/a]$$
$$+\sum_{n=1}^{\infty}\frac{\sinh(n\ln c/b)}{n\pi\epsilon_0 D_{n1}}$$
$$\cdot[\epsilon_{r2}\sinh(n\ln d/a)\cosh(n\ln\rho/d)$$
$$+\epsilon_{r1}\cosh(n\ln d/a)\sinh(n\ln\rho/d)]$$
$$\cdot\cos n(\phi-\theta_{01})\cos(\phi'-\theta_{01})$$
$$\text{for } d\leqslant\rho\leqslant b \tag{7}$$
$$=\frac{\ln c/\rho}{2\pi\epsilon_0 I_0}[\epsilon_{r1}\ln b/d+\epsilon_{r2}\ln d/a]$$
$$+\sum_{n=1}^{\infty}\frac{B_{n1}}{n\pi\epsilon_0 D_{n1}}\sinh(n\ln c/\rho)$$
$$\cdot\cos n(\phi-\theta_{01})\cos n(\phi'-\theta_{01})$$
$$\text{for } b\leqslant\rho\leqslant c \tag{8}$$

where

$$D_{n1}=A_{n1}\epsilon_{r2}\sinh(n\ln c/b)+B_{n1}\epsilon_{r3}\cosh(n\ln c/b) \tag{9}$$
$$A_{n1}=\epsilon_{r2}\sinh(n\ln d/a)\sinh(n\ln b/d)$$
$$+\epsilon_{r1}\cosh(n\ln d/a)\cosh(n\ln b/d) \tag{10}$$
$$B_{n1}=\epsilon_{r2}\sinh(n\ln d/a)\cosh(n\ln b/d)$$
$$+\epsilon_{r1}\cosh(n\ln d/a)\sinh(n\ln b/d) \tag{11}$$

and

$$I_0=\epsilon_{r2}\epsilon_{r3}\ln d/a+\epsilon_{r1}\epsilon_{r3}\ln b/d+\epsilon_{r1}\epsilon_{r2}\ln c/b. \tag{12}$$

Using (2) and (4), the capacitance per unit length of the structure is obtained as

$$\frac{1}{C_1}=\frac{\ln c/b[\epsilon_{r1}\ln b/d+\epsilon_{r2}\ln d/a]}{2\pi\epsilon_0 I_0}$$
$$+\sum_{n=1}^{\infty}\frac{[J_0(n\alpha_1)]^2 B_{n1}\sinh(n\ln c/b)}{n\pi\epsilon_0 D_{n1}} \tag{13}$$

where $J(\cdot)$ is a Bessel function of the first kind of order zero.

Substituting C_1 from (13) into (1), expressions for Z_{c1} and L_1 can be found.

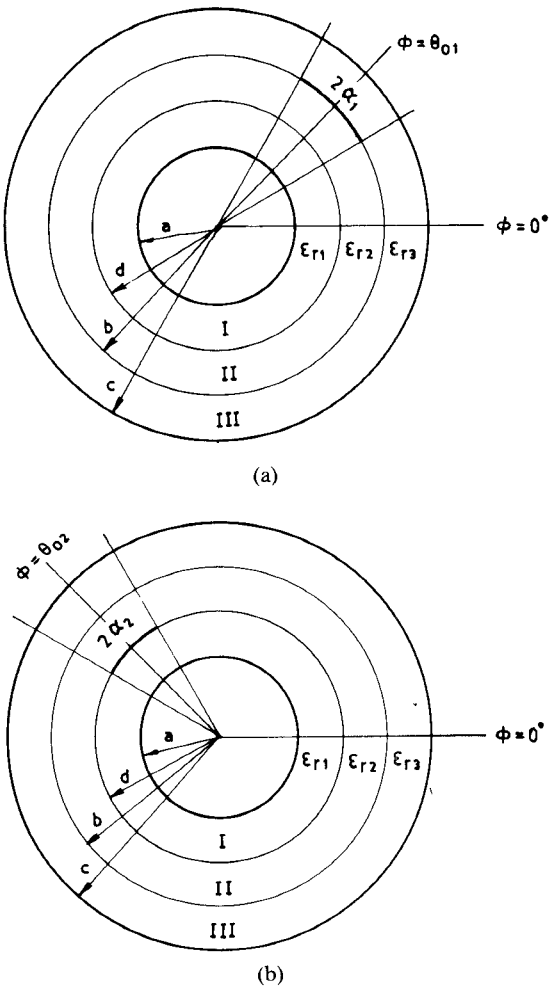

Fig. 1. Cylindrical striplines between two grounded planes filled with layered dielectric. (a) Stripline 1. (b) Stripline 2.

Following a similar procedure with appropriate boundary conditions and a proper charge distribution function, an expression for the capacitance per unit length of the second strip, which is shown in Fig. 1(b), is obtained as

$$\frac{1}{C_2} = \frac{\ln d/a\,[\epsilon_{r3} \ln b/d + \epsilon_{r2} \ln c/b]}{2\pi\epsilon_0 I_0} + \sum_{n=1}^{\infty} \frac{[J_0(n\alpha_2)]^2 B_{n2} \sinh(n \ln d/a)}{n\pi\epsilon_0 D_{n2}} \quad (14)$$

where

$$D_{n2} = A_{n2}\epsilon_{r2} \sinh(n \ln d/a) + B_{n2}\epsilon_{r1} \cosh(n \ln d/a) \quad (15)$$

$$A_{n2} = \epsilon_{r2} \sinh(n \ln c/b) \sinh(n \ln b/d) + \epsilon_{r3} \cosh(n \ln c/b) \cosh(n \ln b/d) \quad (16)$$

$$B_{n2} = \epsilon_{r2} \sinh(n \ln c/b) \cosh(n \ln b/d) + \epsilon_{r3} \sinh(n \ln b/d) \cosh(n \ln c/b). \quad (17)$$

Substituting C_2 and C_{a2} in (1), an expression for Z_{c2} and L_2 is found.

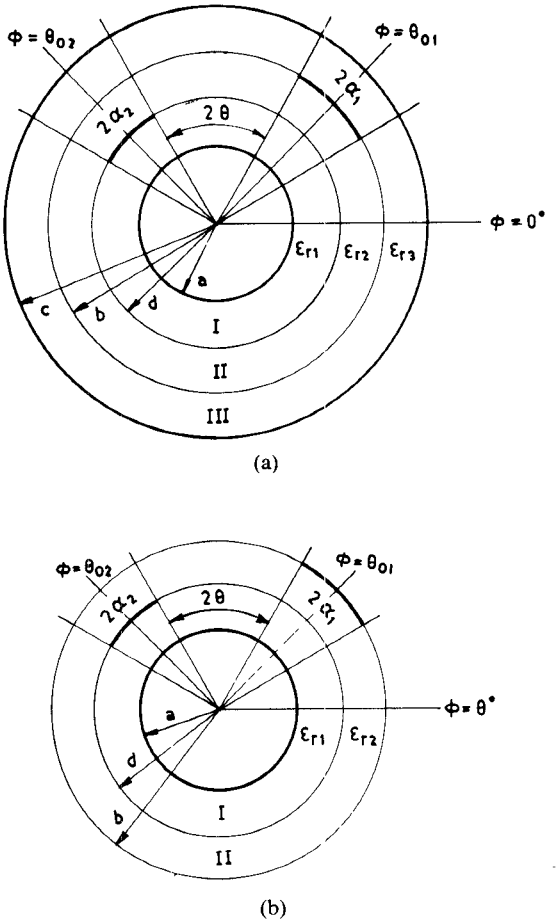

Fig. 2. Coupled cylindrical strips placed at interfaces of layered dielectric. (a) Coupled cylindrical striplines. (b) Coupled cylindrical microstrip lines.

A. Evaluation of Mutual Inductance and Coupling Coefficient

An expression for the mutual inductance is derived for the case of a pair of coupled cylindrical strips, shown in Fig. 2(a), from the relation [13]

$$L_m I_1 I_2 = \frac{1}{\mu_0} \int_v \left(\vec{B}_1 \cdot \vec{B}_2\right) dv \quad (18)$$

where I_1 and I_2 are the currents in first and second strips respectively. $\vec{B}_1$ and $\vec{B}_2$ are the flux densities in the region of interaction due to the strips and μ_0 is the permeability of free space:

$$\vec{B}_1 = \mu_0 \vec{H}_1 \quad (19)$$

$$\vec{B}_2 = \mu_0 \vec{H}_2. \quad (20)$$

Here $\vec{H}_1$ and $\vec{H}_2$ are the magnetic field intensities of the dominant mode fields due to the first and second strips, respectively. Following the procedure given in [14] and carrying out the integration appearing in (18) over the region $\phi = 0°$ to 2π ($\rho = a$ to d, d to b, b to c), an expression for mutual inductance per unit length is ob-

tained as

$$L_m = \frac{\mu_0}{X_1 X_2}\sqrt{\frac{Z_{c1}Z_{c2}}{\eta_1\eta_2}} \cdot \left[\frac{1}{2I_0^2}\left[(\epsilon_{r2}\epsilon_{r3} - \epsilon_{r3}\epsilon_{r1} + \epsilon_{r2}\epsilon_{r1})\ln d/a \ln b/d \ln c/b + \epsilon_{r2}^2 \ln d/a \ln c/b(\ln c/b + \ln d/a)\right] + \sum_{n=1}^{\infty} \frac{J_0(n\alpha_1)J_0(n\alpha_2)}{nD_{n1}D_{n2}} \cos n(\theta_{02} - \theta_{01}) \cdot \left[0.5B_{n2}\epsilon_{r2}\sinh(n\ln c/b)\sinh(2n\ln d/a) + \sinh(n\ln d/a)\sinh(n\ln b/d)\sinh(n\ln c/b) \cdot \left(\epsilon_{r2}^2 \sinh(n\ln d/a)\sinh(n\ln c/b) - \epsilon_{r1}\epsilon_{r3}\cosh(n\ln d/a)\cosh(n\ln c/b)\right) + 0.5B_{n1}\epsilon_{r2}\sinh(n\ln d/a)\sinh(2n\ln c/b)\right]\right] \quad (21)$$

where

$$X_1^2 = \frac{1}{2I_0^2}\left[(\epsilon_{r2}\ln c/b)^2 \ln d/a + (\epsilon_{r1}\ln c/b)^2 \ln b/d + (\epsilon_{r1}\ln b/d + \epsilon_{r2}\ln d/a)^2 \ln c/b\right] + \sum_{n=1}^{\infty} \frac{[J_0(n\alpha_1)]^2}{nD_{n1}^2} \cdot \left[0.5\epsilon_{r2}^2 \sinh^2(n\ln c/b)\sinh(2n\ln d/a) + 0.5\sinh^2(n\ln c/b)\sinh(2n\ln b/d) \cdot \left[\epsilon_{r1}^2\cosh^2(n\ln d/a) + \epsilon_{r2}^2\sinh^2(n\ln d/a)\right] + \epsilon_{r1}\epsilon_{r2}\sinh(2n\ln d/a) \cdot \sinh(n\ln b/d)\sinh(n\ln c/b) + 0.5B_{n1}^2\sinh(2n\ln c/b)\right] \quad (22)$$

and

$$X_2^2 = \frac{1}{2I_0^2}\left[(\epsilon_{r3}\ln b/d + \epsilon_{r2}\ln c/b)^2 \ln d/a + (\epsilon_{r3}\ln d/a)^2 \ln b/d + (\epsilon_{r2}\ln d/a)^2 \ln c/b\right] + \sum_{n=1}^{\infty} \frac{[J_0(n\alpha_2)]^2}{nD_{n2}^2}\left[0.5B_{n2}^2\sinh(2n\ln d/a) + 0.5\sinh^2(n\ln d/a)\sinh(2n\ln b/d) \cdot \left[\epsilon_{r2}^2\sinh^2(n\ln c/b) + \epsilon_{r3}^2\cosh^2(n\ln c/b)\right] + \epsilon_{r2}\epsilon_{r3}\sinh(2n\ln c/b)\sinh^2(n\ln b/d) \cdot \sinh^2(n\ln d/a) + 0.5\epsilon_{r2}^2\sinh^2(n\ln d/a)\sinh(2n\ln c/b)\right]. \quad (23)$$

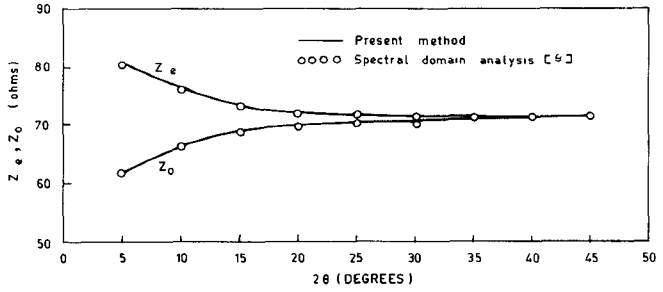

Fig. 3. Variation of even- and odd-mode impedances of a pair of symmetrical coupled coplanar cylindrical striplines as a function of separation angle 2θ with $c/a = 1.5$, $b/a = 1.2$, $\alpha_1 = \alpha_2 = 10°$, $\epsilon_{r1} = \epsilon_{r2} = \epsilon_{r3} = 1$. ——— present method; ∘∘∘∘ spectral-domain analysis [9].

Here η_1 and η_2 are wave impedances and are given by $\eta_1 = 120\pi/\sqrt{\epsilon_{\text{eff1}}}$, $\eta_2 = 120\pi/\sqrt{\epsilon_{\text{eff2}}}$, where ϵ_{eff1} and ϵ_{eff2} are the effective dielectric constants for the first and second strips, respectively.

For the transmission line supporting the dominant TEM mode, the electric and magnetic energies are equal. Thus the mutual inductance and capacitance satisfy the relation

$$L_m I_1 I_2 = C_m V_1 V_2 \quad (24)$$

where $V_1 = I_1 Z_{c1}$ and $V_2 = I_2 Z_{c2}$. The coefficients of electric and magnetic coupling are obtained from the formulas [10]

$$k_L = L_m/\sqrt{L_1 L_2} \quad (25)$$

and

$$k_c = C_m/\sqrt{C_1 C_2}. \quad (26)$$

Maximum coupling is obtained when the coupled length is $\lambda/4$, for which the overall coupling coefficient is given by [14]

$$k = (k_L + k_c)/2. \quad (27)$$

Under the assumption of symmetrically placed strips of equal angular width, calculation of even- and odd mode impedances Z_e and Z_o respectively, is done from the coupling coefficient k as given below [10]:

$$Z_e = [(1+k)/(1-k)]^{1/2} Z_c \quad (28)$$

$$Z_o = [(1-k)/(1+k)]^{1/2} Z_c \quad (29)$$

where $Z_c = Z_{c1} = Z_{c2}$.

B. Computed Results

Numerical results are presented for different cases of coupled cylindrical striplines and microstrip lines. For the sake of comparison, the even- and the odd-mode impedance of a pair of coupled cylindrical striplines with $b/a = d/a$ and $\alpha_1 = \alpha_2$ are calculated as a function of 2θ using the formulas given in (28) and (29). The numerical results thus obtained are compared with those obtained from spectral-domain analysis [9] and are presented in Fig. 3.

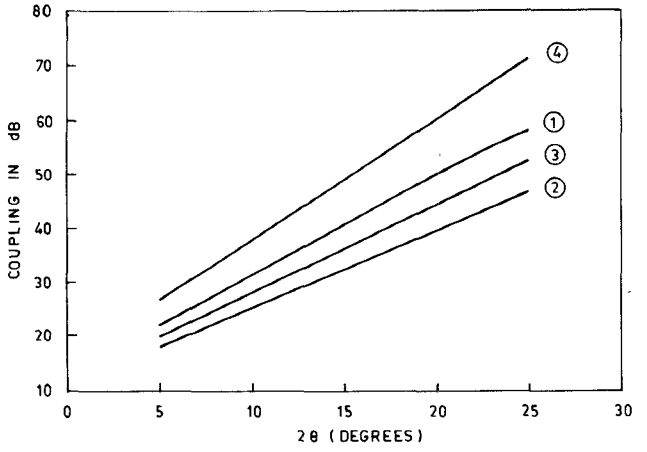

Fig. 4. Variation of coupling as a function of separation angle 2θ of coupled coplanar cylindrical striplines with $c/a = 1.3$, $b/a = d/a = 1.1$:

curve	α_1	α_2	$\epsilon_{r1} = \epsilon_{r2}$	ϵ_{r3}
(1)	5°	10°	2.56	2.56
(2)	5°	10°	2.56	9.6
(3)	5°	10°	2.56	4.6
(4)	20°	10°	4.6	2.56

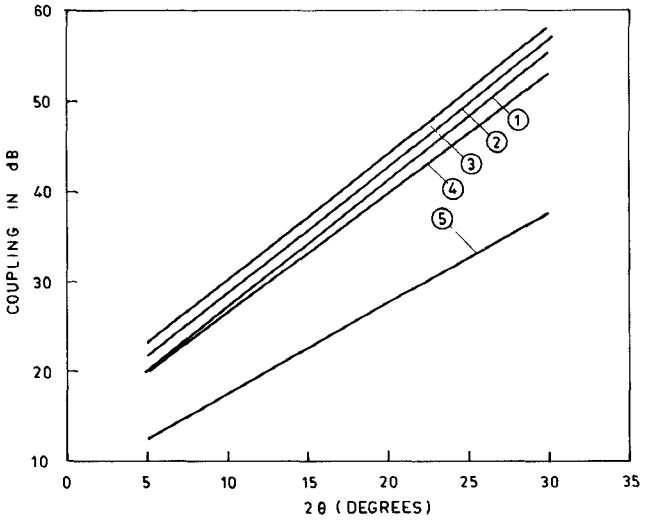

Fig. 5. Variation of coupling as a function of separation angle 2θ of coupled noncoplanar cylindrical striplines with $c/a = 1.4$, $b/a = 1.2$, $d/a = 1.1$:

curve	α_1	α_2	ϵ_{r1}	ϵ_{r2}	ϵ_{r3}
(1)	10°	5°	1	1	1
(2)	10°	10°	1	1	1
(3)	10°	20°	1	1	1
(4)	5°	10°	2.56	4.6	9.6
(5)	10°	5	2.56	4.6	1

Good agreement between results obtained from the two methods can be seen in Fig. 3.

1) Coupled Cylindrical Striplines: Numerical results on coupling in db ($-20\log_{10} k$) as a function of separation angle 2θ are obtained for a pair of coplanar ($b/a = d/a$) cylindrical striplines using the formula given in (27) and presented in Fig. 4 with $c/a = 1.3$, $b/a = d/a = 1.1$. Fig. 5 presents variation of coupling as a function of 2θ for a pair of noncoplanar cylindrical striplines such as are shown in Fig. 2(a) with $c/a = 1.4$, $b/a = 1.2$, and $d/a = 1.1$.

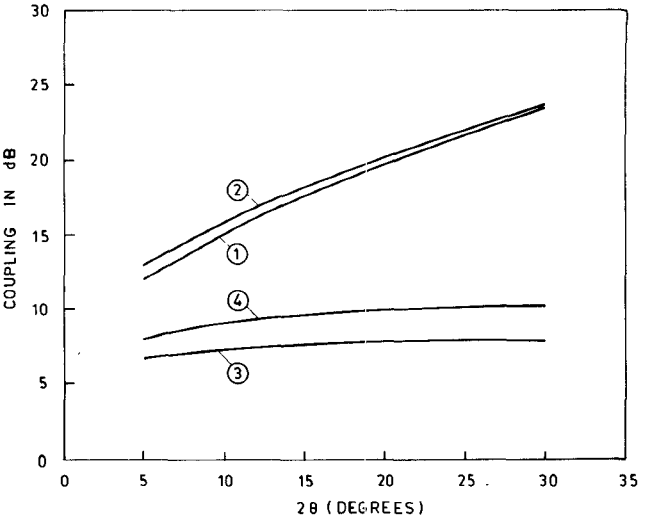

Fig. 6. Coupling versus 2θ of coplanar coupled cylindrical microstrip lines with $b/a = d/a = 1.1$:

curve	α_1	α_2	$\epsilon_{r1} = \epsilon_{r2}$
(1)	10°	10°	1
(2)	10°	20°	1
(3)	10°	20°	2.56
(4)	10°	10°	2.56

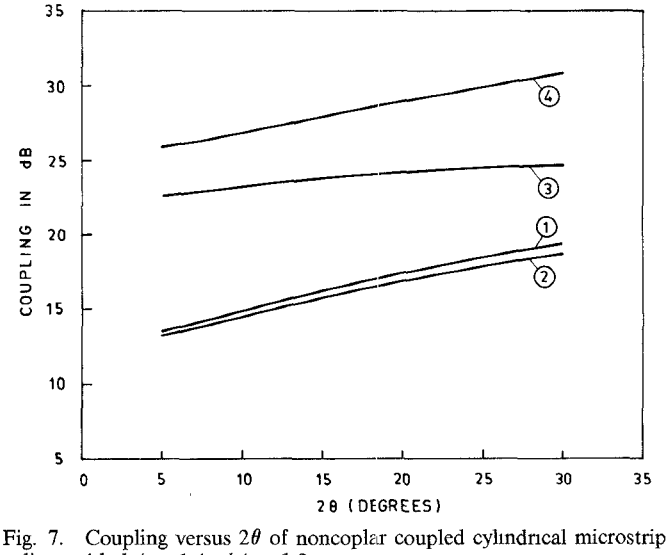

Fig. 7. Coupling versus 2θ of noncoplar coupled cylindrical microstrip lines with $b/a = 1.4$, $d/a = 1.2$:

curve	α_1	α_2	ϵ_{r1}	ϵ_{r2}
(1)	10°	10°	1	1
(2)	10°	20°	1	1
(3)	10°	10°	4.6	2.56
(4)	10°	10°	2.56	1

2) Coupled Cylindrical Microstrip Lines: Cylindrical microstrip lines can be considered as a limiting case of cylindrical stripline with $c \to \infty$ while a, d, b remain finite and $\epsilon_{r3} = 1$. The mutual inductance and thus the mutual capacitance for a pair of coupled cylindrical microstrip lines of the type shown in Fig. 2(b) can be calculated using (21) and (24). Numerical results for the case of coplanar cylindrical microstriplines with $b/a = d/a$ are presented in Fig. 6 for various angular widths of strips and with inhomogeneous dielectric media. Fig. 7 shows variation of

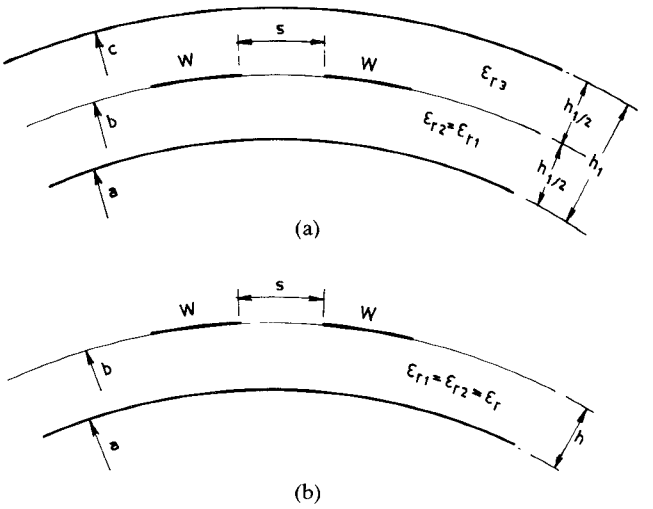

Fig. 8. (a) Cross section of coupled warped striplines. (b) Cross section of coupled warped microstrip lines.

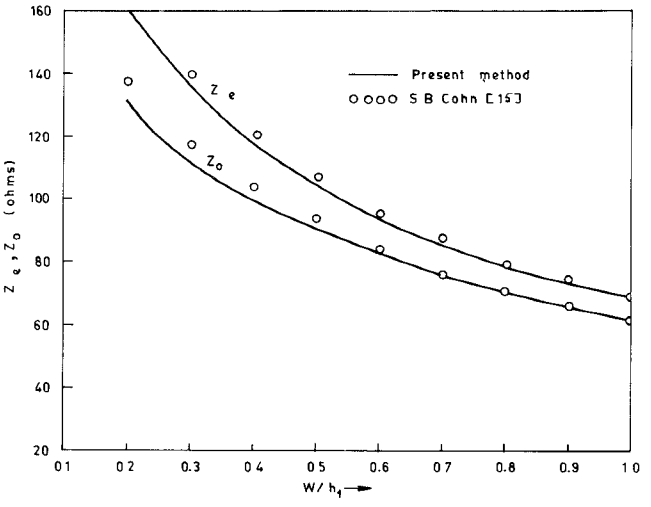

Fig. 9. Variation of even- and odd-mode impedances of warped coupled striplines as a function of W/h_1 with $s/h_1 = 0.5$, $\epsilon_{r1} = \epsilon_{r2} = 1$, $h_1/a = 0.01$. ——— present method; ∘ ∘ ∘ ∘ S. B. Cohn [15].

coupling as a function of 2θ for noncoplanar cylindrical microstrip lines with $b/a = 1.4$ and $d/a = 1.2$.

3) Warped Coupled Striplines and Microstrip Lines: The structure of the warped coupled striplines and microstrip lines to be considered are shown in Figs. 8(a) and (b), respectively, with the notation to be followed. Warped coupled striplines and microstrip lines are considered as limiting cases of cylindrical striplines and microstrip lines, respectively, with $a \to \infty$ and $c - b = b - a = h_1/2$ (for stripline) and $b - a = h$ (for microstrip line) remain finite. The warpage of an otherwise planar structure is indicated by h_1/a and h/a for the stripline and microstrip line cases, respectively. Figs. 9 and 10 show variation of Z_e and Z_o of warped coupled striplines and microstrip lines calculated using (28) and (29) as a function of W/h_1 and W/h, respectively, with $h_1/a = 0.01$ and $h/a = 0.01$. The numerical results for warped coupled lines show good agreement with those for the corresponding planar versions.

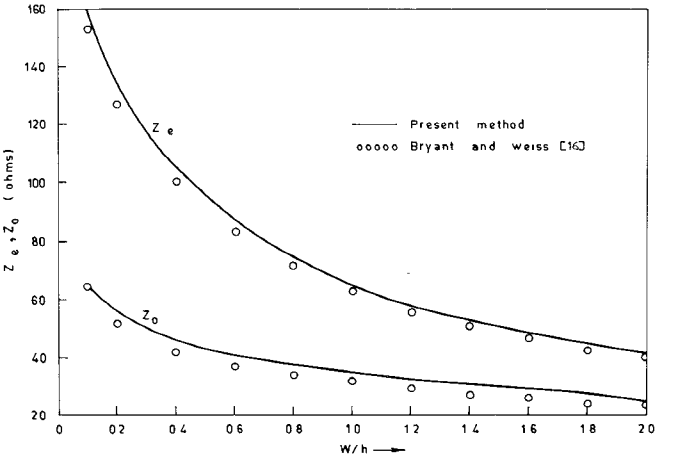

Fig 10. Variation of even- and odd-mode impedances of warped coupled microstrip lines as a function of W/h with $s/h = 0.2$, $\epsilon_r = 10$, and $h/a = 0.01$. ——— present method; ∘ ∘ ∘ ∘ Bryant and Weiss [16].

III. Broad-Side, Edge-Coupled Cylindrical Striplines

The configuration for the three-layer, broad-side, edge-coupled cylindrical stripline to be analyzed is shown in Fig. 11(a) with the notations to be followed. Without loss of generality, the problem can be simplified by assuming that all strips are of equal angular width and are placed symmetrically about the $\phi = 0°$ plane and also about the $\rho = d$ plane, where $d = \sqrt{eb} = \sqrt{ac}$. This structure can support four propagation modes:

(i) even–even mode (ee): magnetic wall at $\phi = 0°$ plane; magnetic wall at $\rho = d$ plane;
(ii) even–odd mode (eo): magnetic wall at $\phi = 0°$ plane; electric wall at $\rho = d$ plane;
(iii) odd–even mode (oe): electric wall at $\phi = 0°$ plane; magnetic wall at $\rho = d$ plane;
(iv) odd–odd mode (oo): electric wall at $\phi = 0°$ plane; electric wall at $\rho = d$ plane.

To compute the propagation parameters of the structure it is sufficient to analyze only one quarter of the structure with appropriate boundary conditions at $\phi = 0°$ and $\rho = d$ corresponding to four different modes.

The scalar potential distribution function satisfies the two-dimensional Laplace equation in cylindrical coordinates [10]:

$$\nabla^2 \psi_{ij}^{\mathrm{I/II}}(\rho, \phi) = 0 \tag{30}$$

where the subscripts ij stand for the ee, eo, oe, or oo mode and I and II stand for region 1 ($a \leqslant \rho \leqslant b$) and region 2 ($b \leqslant \rho \leqslant d$), respectively. Solving (1) and applying appropriate boundary conditions corresponding to the four modes mentioned above, the potential distribution func-

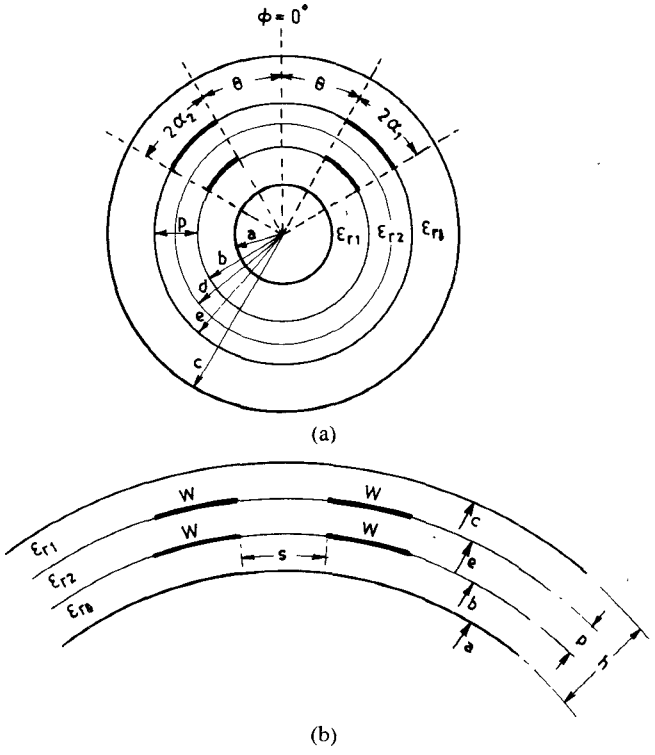

Fig. 11. (a) Cross section of broad-side edge-coupled cylindrical striplines. (b) Cross section of warped broad-side, edge-coupled striplines.

tion for the different modes is obtained as follows:

(i) even–even mode:

$$\psi^{\mathrm{I}}_{ee}(\rho,\phi) = a_{ee}\ln(\rho/a) + \sum_{n=1}^{\infty} a_{nee}\sinh(n\ln\rho/a)\cos(n\phi) \quad (31)$$

$$\psi^{\mathrm{II}}_{ee}(\rho,\phi) = a_{ee}\ln(b/a) + \sum_{n=1}^{\infty} a_{nee}M_{ne}\cosh(n\ln\rho/d)\cos(n\phi) \quad (32)$$

(ii) even–odd mode:

$$\psi^{\mathrm{I}}_{eo}(\rho,\phi) = a_{eo}\ln(\rho/a) + \sum_{n=1}^{\infty} a_{neo}\sinh(n\ln\rho/a)\cos(n\phi) \quad (33)$$

$$\psi^{\mathrm{II}}_{eo}(\rho,\phi) = a_{eo}\frac{\ln b/a}{\ln d/b}\ln\rho/d + \sum_{n=1}^{\infty} a_{neo}M_{no}\sinh(n\ln\rho/d)\cos(n\theta) \quad (34)$$

(iii) odd–even mode:

$$\psi^{\mathrm{I}}_{oe}(\rho,\phi) = \sum_{n=1}^{\infty} a_{noe}\sinh(n\ln\rho/a)\sin(n\phi) \quad (35)$$

$$\psi^{\mathrm{II}}_{oe}(\rho,\phi) = \sum_{n=1}^{\infty} a_{noe}M_{ne}\sinh(n\ln\rho/d)\sin(n\phi) \quad (36)$$

(iv) odd–odd mode:

$$\psi^{\mathrm{I}}_{oo}(\rho,\phi) = \sum_{n=1}^{\infty} a_{noo}\sinh(n\ln\rho/a)\sin(n\phi) \quad (37)$$

$$\psi^{\mathrm{II}}_{oo}(\rho,\phi) = \sum_{n=1}^{\infty} a_{noo}M_{no}\sinh(n\ln\rho/d)\sin(n\theta) \quad (38)$$

where

$$a_{ee} = Q/(\pi\epsilon_0\epsilon_{r1})$$

$$a_{eo} = \frac{Q}{\pi\epsilon_0\left[\epsilon_{r1}+\epsilon_{r2}\dfrac{\ln b/a}{\ln d/b}\right]}$$

$$a_{n_{e(e/o)}} = \frac{2Q_{ne}}{n\pi\epsilon_0 D_{n_{(e/o)}}\sinh(n\ln b/a)}$$

$$a_{n_{o(e/o)}} = \frac{2Q_{no}}{n\pi\epsilon_0 D_{n_{(e/o)}}\sinh(n\ln b/a)}$$

$$Q = \int_0^{\pi} q(b,\phi)\,b\,d\theta$$

$$Q_{ne} = \int_0^{\pi} q(b,\phi)\cos(n\phi)\,b\,d\phi$$

$$Q_{no} = \int_0^{\pi} q(b,\phi)\sin(n\phi)\,b\,d\phi$$

$$D_{ne} = \epsilon_{r1}\coth(n\ln b/a) + \epsilon_{r2}\tanh(n\ln d/b)$$

$$D_{no} = \epsilon_{r1}\coth(n\ln b/a) + \epsilon_{r2}\coth(n\ln d/b)$$

$$M_{ne} = \sinh(n\ln b/a)/\cosh(n\ln d/b)$$

$$M_{no} = \sinh(n\ln b/a)/\sinh(n\ln d/b)$$

$q(b,\phi)$ = charge distribution function on the conducting strip

ϵ_0 = permittivity constant of free space.

The line capacitances for each mode can be obtained from the variational expression [12]

$$\frac{1}{C_{ij}} = \frac{1}{Q^2}\int_0^{\pi}\psi_{ij}(b,\phi)q(b,\phi)\,b\,d\phi. \quad (39)$$

In order to evaluate the line capacitances, the charge distribution function $q(b,\phi)$ has to be specified for each mode. Considering the well-known field singularity at strip edges, the charge distribution function is assumed to be

$$q(b,\phi) = \frac{Q_0}{\sqrt{1-\left[\dfrac{\phi-(\theta+\alpha)}{\alpha}\right]^2}}, \qquad \theta \leqslant \phi \leqslant \theta+2\alpha$$

$$= 0, \qquad \text{otherwise.} \quad (40)$$

Using (31)–(38), substituting (40) into (39), and evaluating the integer, the line capacitances for each mode are

obtained as

$$\frac{\epsilon_0}{C_{ee}} = \frac{\ln b/a}{\pi\epsilon_{r1}} + \sum_{n=1}^{\infty} \frac{2X^2}{n\pi D_{ne}} \tag{41}$$

$$\frac{\epsilon_0}{C_{eo}} = \frac{\ln b/a}{\pi[\epsilon_{r1} + \epsilon_{r2} \ln b/a / \ln d/b]} + \sum_{n=1}^{\infty} \frac{2X^2}{n\pi D_{no}} \tag{42}$$

$$\frac{\epsilon_0}{C_{0_{(e/o)}}} = \sum_{n=1}^{\infty} \frac{2Y^2}{n\pi D_{n_{(e/o)}}} \tag{43}$$

where

$$X = J_0(n\alpha)\cos n(\theta + \alpha)$$

$$Y = J_0(n\alpha)\sin n(\theta + \alpha)$$

$J_0(n\alpha)$ = zeroth-order Bessel function of first kind.

The characteristic impedances Z_{ij} and the effective dielectric constants ϵ_{rij} can be obtained using the following relations:

$$Z_{ij} = \frac{1}{v_0\sqrt{C_{ij}C_{aij}}} \tag{44}$$

$$\epsilon_{rij} = C_{ij}/C_{aij} \tag{45}$$

where C_{aij} is the line capacitance with $\epsilon_{r1} = \epsilon_{r2} = 1$ and v_0 is the velocity of light in free space.

A. Warped Broad-Side, Edge-Coupled Striplines

In order to study the effect of warpage on an otherwise planar structure for broad-side, edge-coupled striplines, we consider the structure shown in Fig. 11(b), where $c - a = h$ and $e - b = p$. Warped broad-side, edge-coupled striplines can be considered as the limiting case of broad-side, edge-coupled cylindrical striplines by assuming that $a \to \infty$, whereas h and p remain finite and α is small. Making use of the approximation $\ln(1+x) \simeq x$ for $x \ll 1$, it can be shown that for the warped case with warpage ratio $h/a \ll 1$, $\ln(b/a) \simeq h/a - (p/2h)(h/a)$ and $\ln(d/b) \simeq (p/2h)(h/a)$ with $\alpha = (W/2h)(h/a)$ and $\theta = (s/2h)(h/a)$.

Substituting the above relations into (41)–(43), the line capacitances for warped broad-side, edge-coupled striplines can be obtained. The characteristic impedances are then calculated using (44).

B. Computed Results

Numerical results for the characteristic impedances of broad-side, edge-coupled cylindrical stripline for the possible four modes are calculated using (41)–(44). Fig. 12 shows the variation of the characteristic impedances (Z_{ee}, Z_{eo}, Z_{oe}, Z_{oo}) as a function of half separation angle θ for $b/a = 1.4$, $p/a = 0.6$, $\alpha = 10°$, $\epsilon_{r1} = 1.0$, and $\epsilon_{r2} = 9.6$. For larger separation angles, it can be seen that Z_{ee} and Z_{oe} approach each other and $Z_{eo} = Z_{oo}$. Variation of characteristic impedances as a function of p/a with $\theta = 5°$, $b/a = 1.4$, $\alpha = 10°$, $\epsilon_{r1} = 1.0$, and $\epsilon_{r2} = 9.6$ is shown in Fig. 13. For large p/a, it can be seen that Z_{ee} and Z_{eo} approach each other and that Z_{oe} and Z_{oo} approach each other. Fig. 14 shows the variation of effective dielectric constants (ϵ_{ree}, ϵ_{reo}, ϵ_{roe}, ϵ_{roo}) as a function of α with $b/a = 1.4$, $p/a = 0.6$, $\theta = 5°$, $\epsilon_{r1} = 1.0$, and $\epsilon_{r2} = 9.6$. With an increase in α, the even–even and odd–even mode effective dielectric constants (ϵ_{ree} and ϵ_{roe}) decrease, while the even–odd and odd–odd mode effective dielectric constants (ϵ_{reo} and ϵ_{roo}) increase.

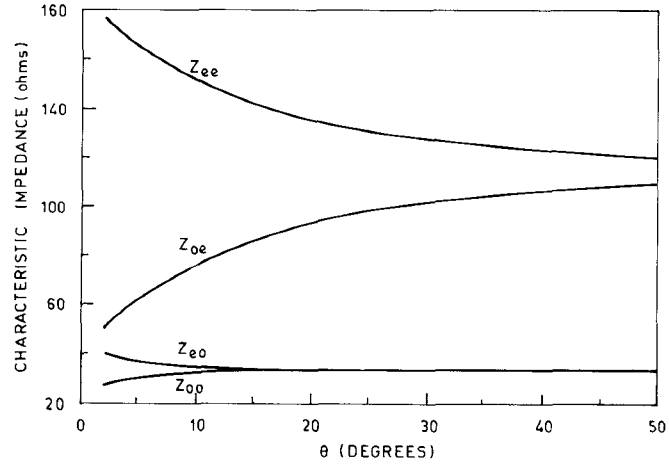

Fig. 12. Variation of characteristic impedances of broad-side, edge-coupled cylindrical striplines as a function of half separation angle θ with $b/a = 1.4$, $p/a = 0.6$, $\alpha = 10°$, $\epsilon_{r1} = 1$, $\epsilon_{r2} = 9.6$.

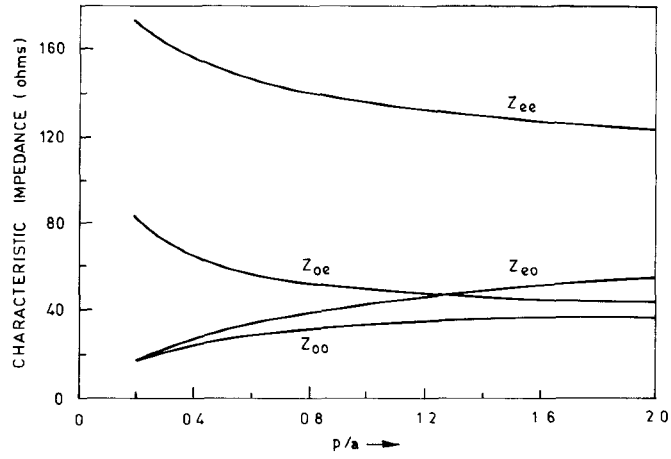

Fig. 13. Variation of characteristic impedances of broad-side, edge-coupled cylindrical striplines as a function of p/a for a fixed separation angle $\theta = 5°$ with $b/a = 1.4$, $\alpha = 10°$, $\epsilon_{r1} = 1$, $\epsilon_{r2} = 9.6$.

The computed characteristic impedances (Z_{ee}, Z_{eo}, Z_{oe}, Z_{oo}) of the broad-side, edge-coupled cylindrical striplines with fixed p/a are plotted as a function of θ in Fig. 15 with $b/a = 1.4$, $p/a = 0.6$, $\alpha = 10°$, $\epsilon_{r1} = 9.6$, and $\epsilon_{r2} = 1$. It is observed that the variations of Z_{ee}, Z_{eo}, Z_{oe}, and Z_{oo} are similar to those obtained in Fig. 12 with $\epsilon_{r1} = 1$ and $\epsilon_{r2} = 9.6$. However, in Fig. 15 it can be seen that Z_{ee} and z_{oe} approach each other faster with an increase in θ. Fig. 16 shows variation of characteristic impedances as a function of p/a for fixed θ, with $\epsilon_{r1} = 9.6$ and $\epsilon_{r2} = 1$. The computed effective dielectric constants are illustrated in Fig. 17 with $\epsilon_{r1} = 9.6$ and $\epsilon_{r2} = 1$ as a function of α. It is seen that with an increase in α, ϵ_{ree} and ϵ_{roe} increase, while ϵ_{reo} and ϵ_{roo} decrease.

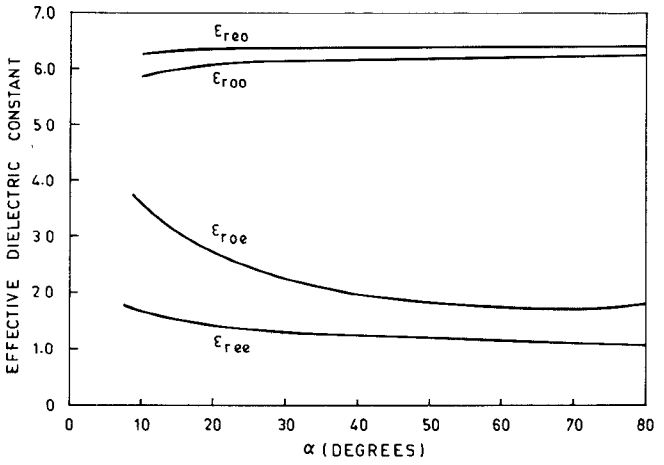

Fig. 14. Variation of effective dielectric constants of broad-side, edge-coupled cylindrical striplines as a function of α with $b/a = 1.4$, $p/a = 0.6$, $\theta = 5°$, $\epsilon_{r1} = 1$, $\epsilon_{r2} = 9.6$.

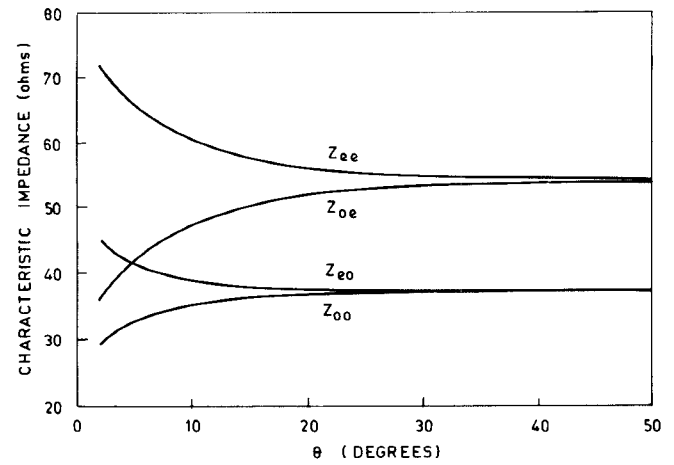

Fig. 15. Variation of characteristic impedances of broad-side, edge-coupled cylindrical striplines as a function of half separation angle θ with $b/a = 1.4$, $p/a = 0.6$, $\alpha = 10°$, $\epsilon_{r1} = 9.6$, $\epsilon_{r2} = 1$.

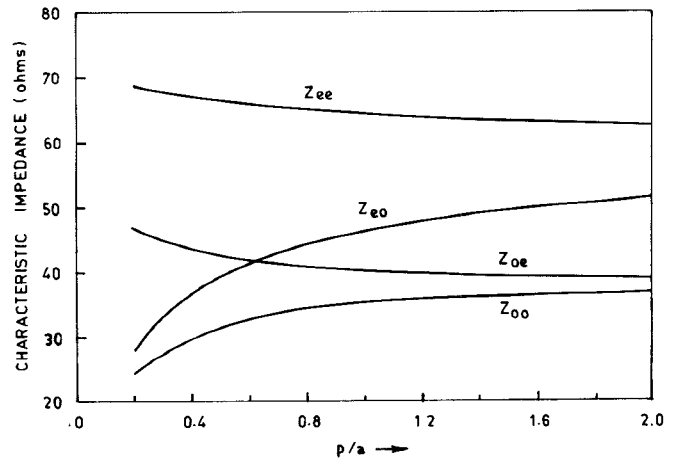

Fig. 16. Variation of characteristic impedances of broad-side, edge-coupled cylindrical striplines as a function of p/a for a fixed separation angle $\theta = 5°$ with $b/a = 1.4$, $\alpha = 10°$, $\epsilon_{r1} = 9.6$, $\epsilon_{r2} = 1$.

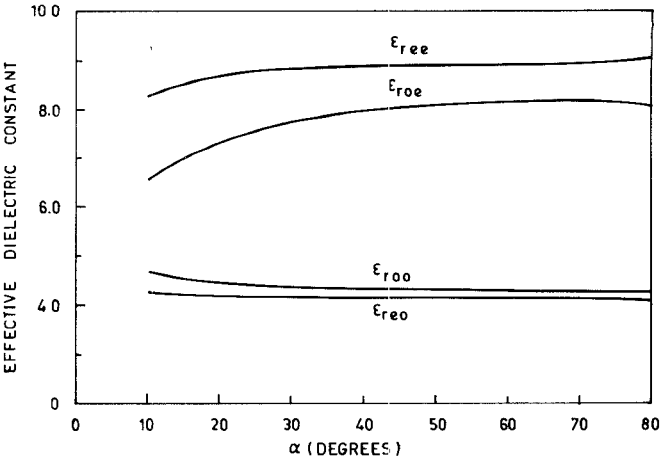

Fig. 17. Variation of effective dielectric constants of broad-side, edge-coupled cylindrical striplines as a function of α with $b/a = 1.4$, $p/a = 0.6$, $\theta = 5°$, $\epsilon_{r1} = 9.6$, $\epsilon_{r2} = 1$.

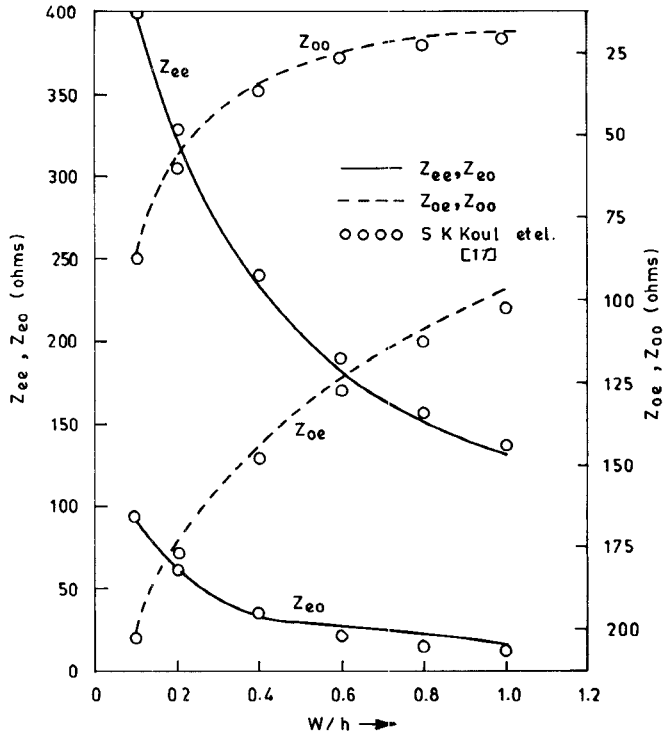

Fig. 18. Characteristic impedance versus W/h for warped broad-side edge-coupled striplines with $p/h = 0.1$, $s/h = 0.2$, $\epsilon_{r1} = \epsilon_{r2} = 1$, $h/a = 0.01$.

To study the effect of warpage on an otherwise planar broad-side, edge-coupled stripline structure, numerical results for cylindrically warped broad-side, edge-coupled striplines are computed as suggested in the previous section, using (41)–(44). The results for characteristic impedances Z_{ee}, Z_{eo}, Z_{oe}, and Z_{oo} of warped broad-side, edge-coupled striplines are calculated and presented in Fig. 18. For the sake of comparison, the numerical results obtained by Koul *et al.* [17] for a planar structure are also presented. It can be seen that for a warpage with warpage ratio $h/a = 0.01$, there is good agreement between the two sets of results.

IV. Conclusions

An expression for coupling is derived which can be applied for the general case of a pair of coupled cylindrical strip and microstrip lines with multilayered dielectrics. The particular advantage of the analysis presented in this paper is that the same formulation can be applied to different structures resulting from arbitrary locations of strips and choices of dielectrics. The propagation parameters of a symmetric broad-side, edge-coupled cylindrical stripline structure are also studied. It is observed that the values of the even–even mode and odd–even mode effective dielectric constants with inhomogeneous dielectric media are different from those of even–odd mode and odd–odd mode effective dielectric constants. The effect of warpage due to environmental changes on an otherwise planar structure is also studied. For a warpage ratio of $h/a \ll 1$, it is seen that the numerical data obtained for warped coupled stripline structures are close to those obtained for planar coupled stripline structures.

References

[1] Y. C. Wang, "Cylindrical and cylindrically warped strip and microstrip lines," *IEEE Trans. Microwave Theory Tech.*, vol. MTT-26, pp. 20–23, Jan. 1978.

[2] K. K. Joshi and B. N. Das, "Analysis of elliptic and cylindrical strip lines using Laplace's equation," *IEEE Trans. Microwave Theory Tech.*, vol. MTT-28, pp. 381–386, Apr. 1980.

[3] K. K. Joshi, J. S. Rao, and B. N. Das, "Characteristic impedance of nonplanar strip lines," *Inst. Elec. Eng., pt. H*, vol. 127, pp. 287–291, Aug. 1980.

[4] B. N. Das, A. Chakrabarty, and K. K. Joshi, "Characteristic impedance of elliptic cylindrical strip and microstrip lines filled with layered substrate," *Proc. Inst. Elec. Eng., pt. H*, vol. 130, pp. 245–250, June 1983.

[5] L. R. Zeng and Y. Wang, "Accurate solutions of elliptic and cylindrical strip lines and microstrip lines," *IEEE Trans. Microwave Theory Tech.*, vol. MTT-34, pp. 259–265, Feb. 1986.

[6] C. J. Reddy and M.D. Deshpande, "Analysis of cylindrical strip line with multilayer dielectrics," *IEEE Trans. Microwave Theory Tech.*, vol. MTT-34, pp. 701–706, June 1986.

[7] B. N. Das and K. V. S. V. R. Prasad, "Even and odd mode impedances of coupled elliptic arc strips," *IEEE Trans. Microwave Theory Tech.*, vol. MTT-32, pp. 1475–1479, Nov. 1984.

[8] C. H. Chan and R. Mittra, "Analysis of a class of cylindrical multiconductor transmission lines using an iterative approach," *IEEE Trans. Microwave Theory Tech.*, vol. MTT-35, pp. 415–423, Apr. 1987.

[9] M. D. Deshpande and C. J. Reddy, "Spectral domain analysis of single and coupled cylindrical striplines," *IEEE Trans. Microwave Theory Tech.*, vol. MTT-35, pp. 672–675, July 1978.

[10] M. K. Krage and G. I. Haddad, "Characteristics of coupled microstrip lines—I: Coupled mode formulation of inhomogeneous lines, and II: Evaluation of coupled line parameters," *IEEE Trans. Microwave Theory Tech.*, vol. MTT-18, pp. 217–228, Apr. 1970.

[11] S. Ramo, J. R. Whinnery and T. V. Duzer, *Fields and Waves in Communication Electronics*. New Delhi: Wily Eastern Private Ltd., 1970.

[12] R. E. Collin, *Field Theory of Guided Waves*. New York: McGraw-Hill, 1960.

[13] W. R. Smythe, *Static and Dynamic Electricity*. New York: McGraw-Hill, 1968, pp. 333.

[14] B. N. Das and K. V. S. V. R. Prasad, "A generalized formulation of electromagnetically coupled strip lines," *IEEE Trans. Microwave Theory Tech.*, vol. MTT-32, pp. 1427–1433, Nov. 1984.

[15] S. B. Cohn, "Shielded coupled strip transmission lines," *IEEE Trans. Microwave Theory Tech.*, vol. MTT-3, pp. 29–38, Oct. 1955.

[16] T. G. Bryant and J. A. Weiss, "Parameters of microstrip transmission lines and of coupled pair of microstrip lines," *IEEE Trans. Microwave Theory Tech.*, vol. MTT-16, pp. 1021–1027, Dec. 1968.

[17] S. K. Koul and B. Bhat, "Broad side, edge coupled symmetric strip transmission lines," *IEEE Trans. Microwave Theory Tech.*, vol. MTT-30, pp. 1874–1880, Nov. 1982.

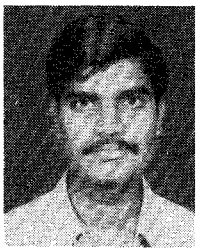

C. Jagadeswara Reddy was born in Nellore, India, on April 17, 1962. He received the B.Tech. degree in electronics and communication engineering from the Regional Engineering College, Warangal, India, in 1983 and the M.Tech. degree in microwave and optical communication engineering from the Indian Institute of Technology, Kharagpur, in 1986. He recently received the Ph.D. degree from the Indian Institute of Technology, Kharagpur. His thesis was on the characteristics of cylindrical strip/microstrip lines.

In 1987, he joined the Society for Applied Microwave Electronics Engineering and Research (SAMEER), Bombay, where he has been engaged in the development of radar antennas.

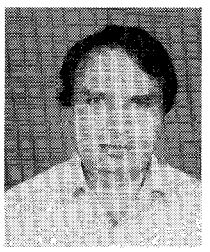

Manohar D. Deshpande was born in Lohgaon, India, on June 3, 1948. He received the B.E. (electrical) degree in 1970 from V.R.C.E., Nagpur, and the M.Tech. and Ph.D. degree in microwave and radar engineering from the Indian Institute of Technology, Kharagpur, in 1972 and 1980, respectively.

In 1975, he joined the faculty of the Indian Institute of Technology, Kharagpur, where he currently holds the position of Assistant Professor of Electronics and Electrical Communication Engineering. At present, he is working at NASA-Langley Research Center, Hampton, VA, as Senior NRC Resident Research Associate on leave from the Indian Institute of Technology, Kharagpur.